Coast. Sed. 1999.

DEPTH-INTEGRATED SAND TRANSPORT IN THE SURF ZONE

Bart T. Grasmeijer[1], Dang Huu Chung[2] and Leo C. van Rijn[3]

Abstract: In this paper the relative contributions of the various transport components to the total depth-integrated transport rates are demonstrated. From wave tunnel measurements it appeared that the near-bed transport rate could be predicted with reasonable accuracy using a relatively simple bedload transport formulation. Suspended load transport rates ($q_{suspended}$) were measured in a large wave flume and in the field using optical and acoustical instruments. The time-averaged suspended transport component and the high-frequency suspended transport component were found to be the most important components in determining the direction and the magnitude of the net suspended transport rate. The computed near-bed transport rate was found to be of the same order of magnitude as the net suspended transport rate and sometimes even larger. The high-frequency suspended transport component could be predicted with reasonable accuracy using the method of Houwman and Ruessink (1996).

INTRODUCTION

The morphological behaviour of nearshore bars and the associated net sediment transport rates under the influence of wave action and wave- and tide-induced currents are poorly understood. The generation and maintenance of nearshore bars are commonly associated with the shoaling and breaking of high-frequency waves and the generation of low-frequency wave effects in the surf zone. Field and laboratory

1) Institute for Marine and Atmospheric Research Utrecht, Utrecht University, P.O. Box 80.115, 3508 TC Utrecht, The Netherlands. Teleph: +31.30.2535735; e-mail: B.Grasmeijer@geog.uu.nl.
2) Institute of Mechanics, 224 Doi Can, Hanoi, Vietnam. Teleph: 84-4-8326138; email: dhchung@im01.ac.vn
3) Delft Hydraulics, P.O.Box 117, 2600 MH Delft, The Netherlands. Teleph: +31.15.2858585; e-mail: Leo.vanRijn@wldelft.nl.

measurements indicate that flux contributions by the mean flow and the oscillatory wave motions at both high and low frequencies are highly variable not only in magnitude, but also in direction. The fluxes also vary significantly with elevation above the bed (Vincent and Green, 1990; Osborne and Greenwood, 1992; Osborne and Vincent, 1996).

In the present paper the relative contributions of the various transport components to the total depth-integrated transport rate are demonstrated. Laboratory measurements were performed in the oscillating water tunnel of Delft Hydraulics in order to relate the near-bed transport rate to a simple transport formulation. Measurements in the Delta Flume were performed to get information on the wave-related suspended sand transport rate. Estimates are given of the suspended transport and bed load transport in the unmeasured zone near the bed. The high-frequency suspended load transport rates measured in the Delta flume are compared with a formulation proposed by Houwman and Ruessink (1996). Field measurements near the coast of Egmond aan Zee, the Netherlands, were conducted in order to study the depth-integrated sand transport rates under natural conditions at different locations across an inner nearshore bar.

DEFINITIONS

The depth-integrated instantaneous sand transport is defined as the sum of bed load transport and suspended load transport. The bed-load transport is the transport of sediment in a layer near the bed with thickness equal to the thickness of the wave boundary layer δ (order of 0.01-0.02 m).

$$q_{bed} = \int_0^{\delta} UCdz \tag{1}$$

The suspended load transport is defined as the integration of instantaneous velocity and concentration above δ.

$$q_{suspension} = \int_{\delta}^{h} UCdz = \int_{\delta}^{h} (uc)_{mean}\, dz + \int_{\delta}^{h} (uc)_{hf}\, dz + \int_{\delta}^{h} (uc)_{lf}\, dz \tag{2}$$

The first term represent the time-averaged transport, the second term the high frequency transport and the third term the low-frequency transport, with $U = u + u_{hf} + u_{lf}$ and $C = c + c_{hf} + c_{lf}$. The frequency that was used to filter high and low frequencies were 0.1 Hz ($\frac{1}{2}f_p$) for laboratory conditions and 0.05 Hz for field conditions. Instantaneous velocities and concentrations can be measured in a number of points above the bed by acoustical and optical instruments.

BED LOAD TRANSPORT

Measurement of instantaneous velocities and concentrations in the bedload layer are of crucial importance to determine the depth-integrated transport rates. It is however hardly possible to measure these transport rates with the available measurement techniques, not even in flume conditions. Therefore, another approach was used based on large-scale wave tunnel experiments to find a suitable bed load transport formula in line with the work of Ribberink (1998).

Wave tunnel experiments

Laboratory measurements were performed in the oscillating water tunnel (Ribberink and Al-Salem, 1991, 1992) of Delft Hydraulics. The tunnel has a width of 0.3 m and a height above the sand bed of 0.8 m. Two different test series were performed using two different sediment sizes with a median diameter of 0.19 mm and 0.12 mm respectively. Regular asymmetric wave motion (second order Stokes), irregular wave motion, and regular symmetric wave motion with a following current were generated. The test conditions are given in Table 1.

Table 1. Test conditions wave tunnel measurements

Test	Condition	Mean current at 0.1 m to bed (m/s)	$U_{max,on}$ $U_{1/3,on}$ (m/s)	$U_{max,off}$ $U_{1/3,off}$ (m/s)	Period T (s)	Bed type and D_{50} (mm)	Total net sand transport (kg/s/m)
B2	Irregular Jonswap	0	0.84	0.48	6.5	plane 0.21	0.009
B7	Regular Asym.	0	0.98	0.51	6.5	plane 0.21	0.033
B8	Regular Asym.	0	1.28	0.66	6.5	plane 0.21	0.102
B_{00}	Regular Asym.	0	0.52	0.33	6.5	ripples H=3 cm L=8 cm 0.21	not measured
J1	Regular Symm.	0.24	1.06	1.06	7.2	plane 0.21	0.104
E2	Regular Symm.	0.23	1.47	1.47	7.2	plane 0.21	?
E4	Regular Symm.	0.44	0.95	0.95	7.2	plane 0.21	0.188
H2	Regular Symm.	0.23	0.68	0.68	7.2	plane 0.13	0.042
H5	Regular Symm.	0.23	1.3	1.3	7.2	plane 0.13	0.11
H8	Regular Symm.	0.44	0.67	0.67	7.2	plane 0.13	0.105

The total load transport rate (q_{total}) was determined during previous experiments in the wave tunnel using a mass conservation technique (Janssen et al, 1996). The transport rate in the suspension layer ($q_{suspension}$) was measured using an OBS-transport meter consisting of three OBS's at 0.025, 0.045 and 0.095 m above the bed. The transport rate in the unmeasured zone near the bed was determined from $q_{bed} = q_{total} - q_{suspension}$.

Time-averaged concentrations measured with the OBS's were compared with time-averaged concentrations measured with a pump sampling system. The pump sampling system consisted of nine intake tubes at elevations between 0.005 to 0.26 m above the bed. An example of the vertical distribution of time-averaged concentrations (test H5)

measured with OBS's and pump sampler is shown in Figure 1. The concentrations measured with the OBS and the concentrations measured with the pump sampler were found to be of the same order of magnitude. On an average, the OBS sensors gave values that were 15% larger in case of coarse sand and 29% larger in case of fine sand than the values determined with the pump sampler. The largest differences were found for test H2 in which the concentration gradient was relatively large (fine sand, small orbital velocity and weak current compared to other tests). Velocities were measured using an EMF and a laser Doppler velocity meter.

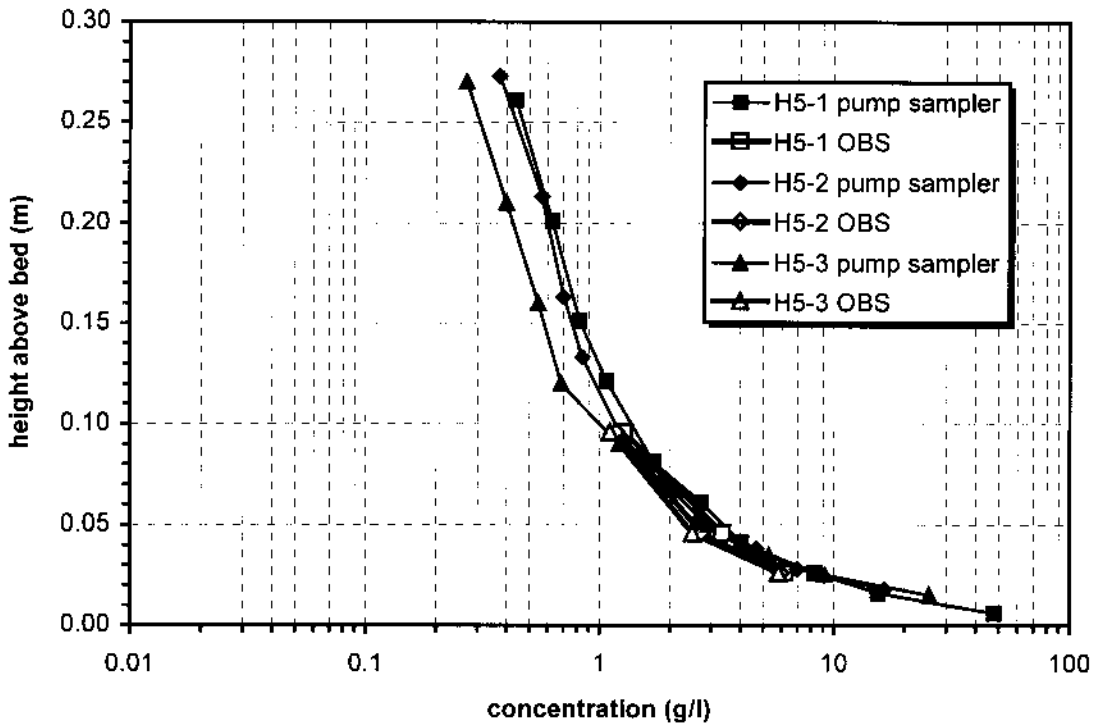

Fig. 1. Vertical distribution of time-averaged concentration

Comparison of the total load transport rates (q_{total}) and the transport rates based on EMF and OBS data ($q_{suspension}$) showed the latter to be relatively small. It was found that the absolute values of $q_{suspension}$ make less than 10% (on an average: 4%) of the total net transport rate q_{total}. This indicates that more than 90% of the total transport rate takes place in the unmeasured zone near the bed ($z < 0.025$ m). This is consistent with findings by Ribberink and Al-Salem (1991, 1992) in the wave tunnel.

It was tried to relate the transport rate in the unmeasured zone near the bed to a simple transport formulation of the form $q = q(\theta)$, in which q is the instantaneous transport rate during the wave cycle in sediment volume per unit width and time and θ is the instantaneous dimensionless bed shear stress. The instantaneous bedload transport rate is expressed as (see Ribberink, 1998):

$$\frac{< q_{bed} >}{\sqrt{(s-1)gD_{50}^3}} = m < (|\theta'| - \theta_{cr,shields})^n \frac{\theta'}{|\theta'|} > \qquad (3)$$

in which:

<...>	: time-averaging	
q_{bed}	: instantaneous bedload transport rate	[$m^3/m/s$]
s	: relative density of sediment (ρ_s/ρ)	[-]
g	: acceleration of gravity	[m^2/s]
D_{50}	: median grain size of sediment	[m]
m, n	: coefficients	[-]
θ'	: instantaneous dimensionless bed shear stress	[-]
$\theta_{cr, shields}$	: critical dimensionless bed shear stress	[-]

Generally the same procedure is followed as described by Ribberink 1998 with the exception of the iterative procedure in determining the bed roughness, which is not used in the present study. In the present study the bed roughness is estimated with $k_s = 3D_{90}$. The threshold value $\theta_{cr, shields}$ is calculated according to the classical shields curve.

Ribberink 1998 found m = 11 and n = 1.65 using datasets from various researchers. The validity range expressed in terms of the Shields parameters and the grain sizes was given as: $\theta_{cr, shields}$ = 0.1 - 7, D_{50} = 0.2 – 3.8 mm. However, for steady flows the bed-load formula showed a tendency of increasing m for increasing Shields number. The Shields number and grain diameter for the present experiments are relatively small: $\theta_{cr,shields}$ = 0.05 - 0.08, D_{50} = 0.13 – 0.19 mm. In the present study an alternative current-related friction coefficient is used than that proposed by Ribberink 1998. Therefore, different values for the coefficients m and n may be expected. As a first approximation the following values were used: m = 5, n = 1.65.

A comparison between calculated and measured transport rates for the unmeasured zone near the bed is shown in Figure 2. It can be observed from this figure that the near-bed transport rates are rather accurately predicted using the method described above. On an average the calculated transport rates are 7% smaller than the measured transport rates. The standard error is less than 20%. Largest differences are found for test B8 (large asymmetrical orbital velocities; no current). The calculated near-bed transport rate is 44% smaller than measured near-bed transport rate in this case.

Another n coefficient of 1.8 was also used in this study. Using m = 5 and n = 1.8 improves the results. The calculated transport rates are 3% larger (on an average) than the measured values in this case. The standard error is less than 20%. The largest difference is found for test B8 in which the calculated transport rate is 36% smaller than the measured transport rate. In the remaining of this paper these values for m and n (m=5 and n=1.8) will be used to calculated the near bed transport rate.

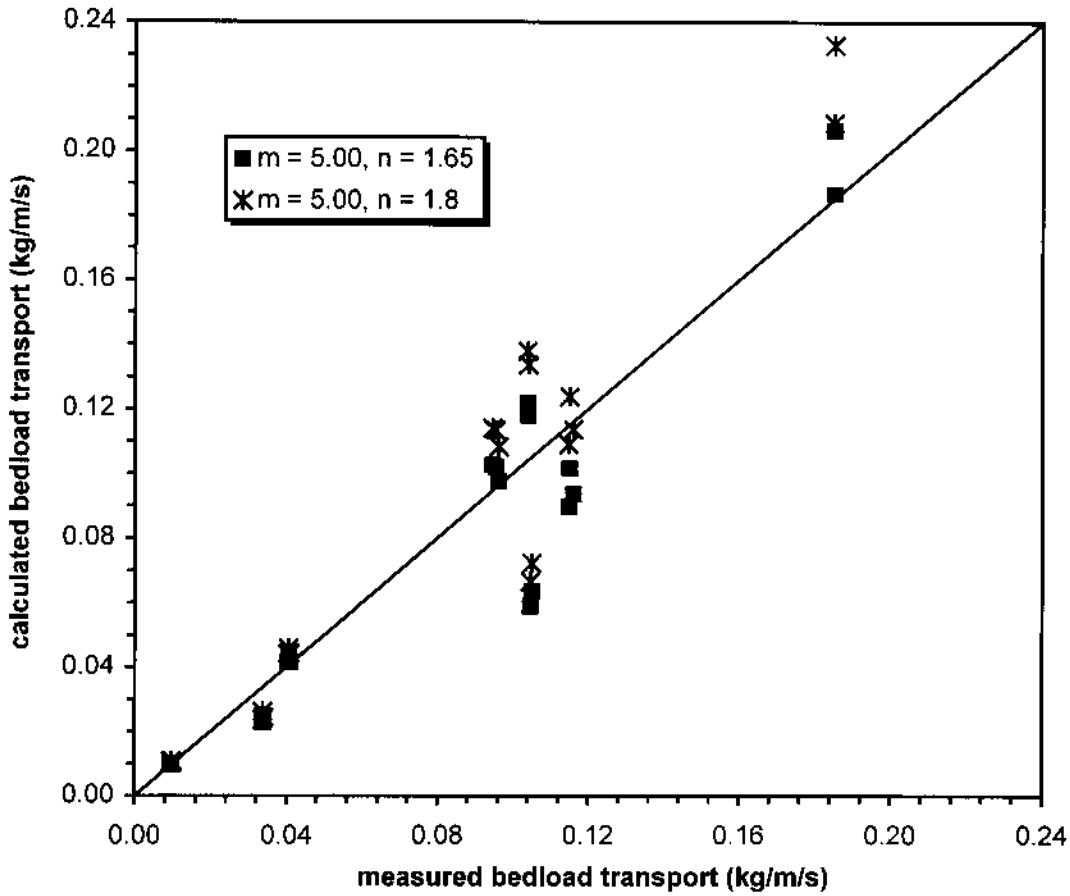

Fig. 2. Calculated and measured bedload transport rates

SUSPENDED LOAD TRANSPORT

Delta flume experiments

To get information on the wave-related suspended load sand transport, experiments were performed in the Delta flume of DELFT HYDRAULICS (Dang Huu et al. 1999) The high-frequency oscillatory suspended load transport rates measured in the Delta flume were compared with a formulation proposed by Houwman and Ruessink (1996). The Delta Flume has a total length of 233 meters, a depth of 7 meters and a width of 5 meters. A piston activated wave board on one side of the flume generates the waves. A horizontal sand bed was placed in the flume over a length of about 40 m (Figure 3).

An acoustical instrument (ASTM) was used to measure the instantaneous fluid velocities and sand concentrations at five points above the bed simultaneously. The measured mean values (time-averaged over 15 min.) of the ASTM were compared to the concentrations measured with a pump sampler.

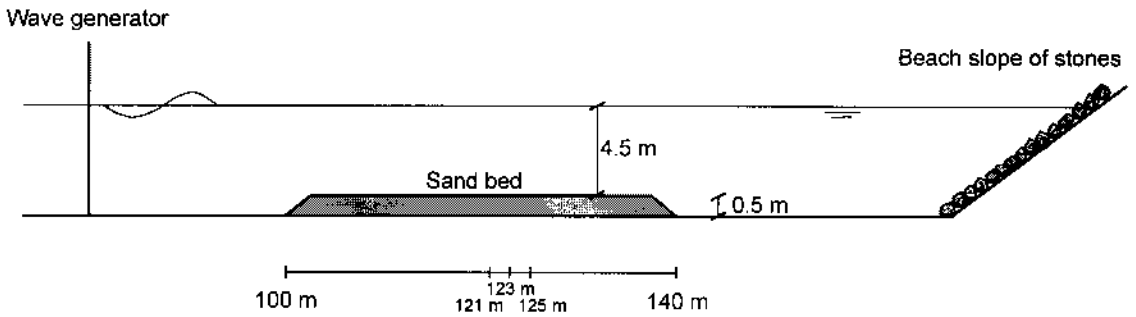

Fig. 3. Sketch of Delta Flume

The pump sampler consisted of pumping system and two pairs of 5 intake tubes. The first pair was attached to the five ASTM sensors. The second pair of 5 intake tubes was attached to a separate system, approximately 2 m away from the ASTM. The intake tubes of 3 mm internal diameter were connected to the pumps by plastic hoses. The lowest intake tubes were placed at about 0.07 m above the bed, with the intake openings placed in a direction transverse to the plane of orbital motion. The intake velocity was about 1 m/s, satisfying sampling requirements. The 10 liter samples were collected in calibrated buckets. The pump sampler was operating for 15 minutes giving an average concentration over the measuring time. An example of the vertical distribution of time-averaged concentration measured with the two pairs of intake tubes is shown in Figure 4.

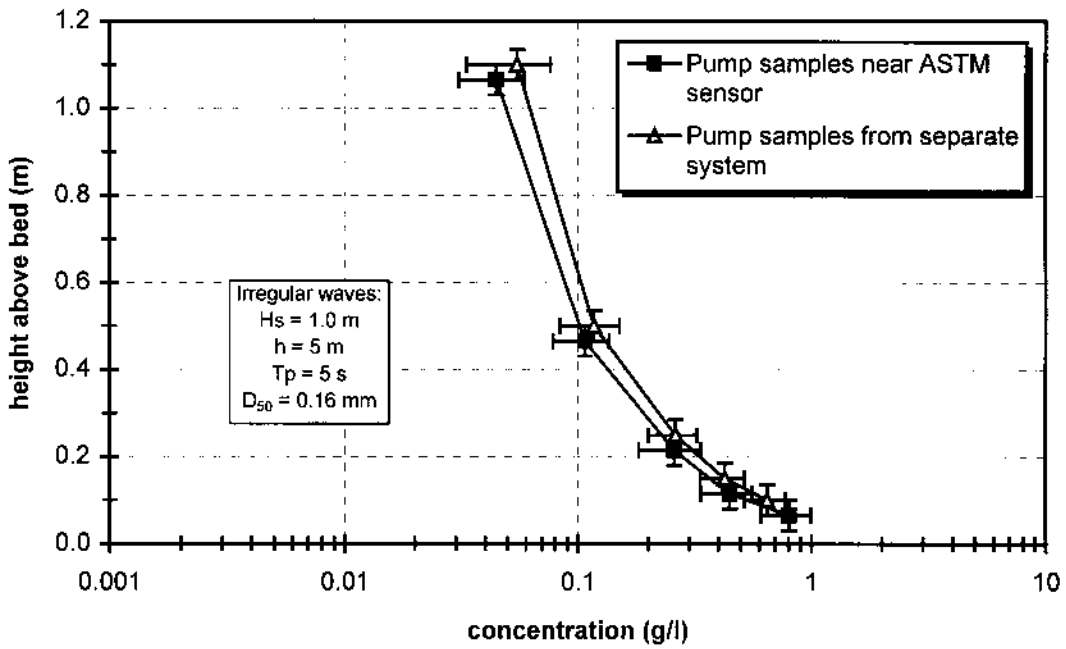

Fig. 4. Vertical distribution of time-averaged concentration measured with pump sampler.

Other instruments were used to obtain additional data of velocities and concentrations. The instruments were mounted in a tripod, which was placed on the sand bed at location x = 125 m (Figure 3). During each test the instruments were operated for about 15 minutes to sample over a representative wave record. The experiments are two-dimensional, in the sense that the waves are normal to the sand

bed (cross-shore experiment with no longshore component) but local processes are three dimensional due to the generation of bedforms (ripples).

Three different wave conditions were generated during the test series, one regular waves condition (H = 1.0 m) and two irregular wave conditions ($H_{1/3}$ = 1.0 and 1.25 m). The measurement program consisted of five days of testing in July and August 1997. During the first two days of the program (July 1997) tests were performed using relatively coarse sand with a median diameter of 0.33 mm. During the second part of the program (August 1997) finer sand was used with a median diameter of 0.16 mm. Each test was repeated at least three times. In total 48 tests were performed.

Transport components

Measurements of instantaneous concentrations and velocities were analyzed in terms of mean (time-averaged) and oscillating components, as described before. An example of the vertical distribution of transport rates for a test with coarse sand (D_{50} = 0.33 mm) and irregular waves (H_s = 1.25 m), is given in Figure 5. It can be observed that the time-averaged transport rate (Qxa) is onshore directed at the lowest three measurement points (z < 0.4 m) and offshore directed (although small) at higher elevations above the bed. The high-frequency transport rate (Qxss) is onshore directed at the lowest three measurement points and negligible at higher elevations. The low-frequency transport rate (Qxll) is offshore directed at the lowest three measurement points and almost zero at higher elevations above the bed. The components of interaction between high and low frequencies (Qxsl and Qxls) are very small and can be ignored. It can be observed from Figure 5 that the high-frequency component is relatively large compared to the other transport components. Consequently, the net transport rate (Qx) is mainly determined by the high-frequency transport component.

In most tests the high-frequency suspended transport rate was measured in the layer between z = 0.075 m and 1.075 m (layer 1) above the bed, using the ASTM. The high-frequency transport component in the unmeasured zone below z = 0.075 m was assumed to consist of high-frequency suspended transport in the layer between z = 0.01 m and 0.075 m (layer 2) and of high-frequency bedload transport in the layer below z = 0.01 m (layer 3). The high-frequency suspended transport in layer 2 was estimated from the measured high-frequency suspended transport in layer 1 using extrapolation. The high-frequency bedload transport was estimated by substituting instantaneous high-frequency velocities near the bed into Eq.(3) and time averaging. Figure 6 shows results of high-frequency transport component in layer 1, 2 and 3. Based on these results, it can be concluded that the high-frequency transport component in the unmeasured zone (layer 2 and 3) is of the same order or larger than the high-frequency suspended transport in the measured zone (layer 1). These results clearly show that accurate determination of the depth-integrated transport requires measurements of instantaneous velocity and concentration as close as possible to the bed upto 0.01 or 0.02 m above the bed. Therefore, the instrument arrangement used at the field site of Egmond aan Zee (see below) was improved to allow measurements of velocity and concentration as close as 0.02 m above the bed.

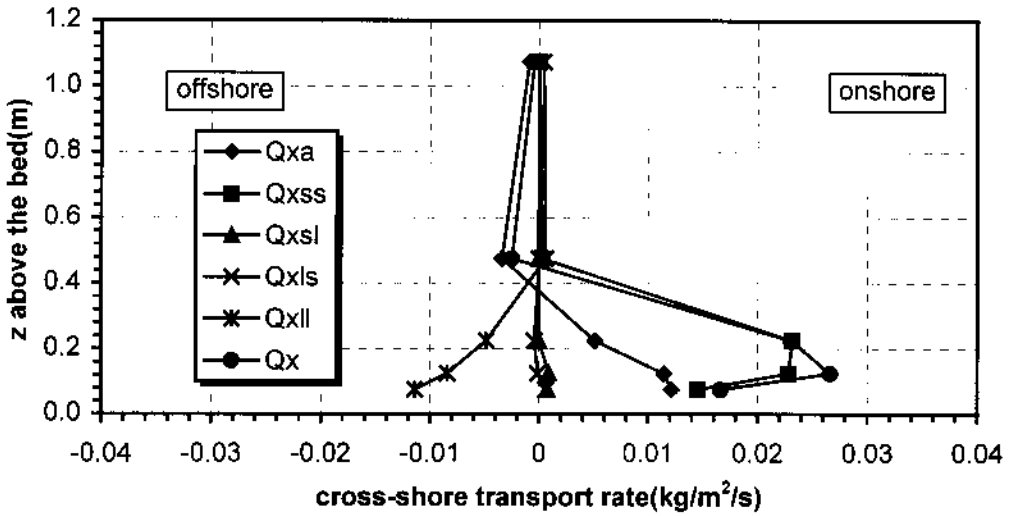

Fig. 5. Vertical distribution of transport rates (test B2A).

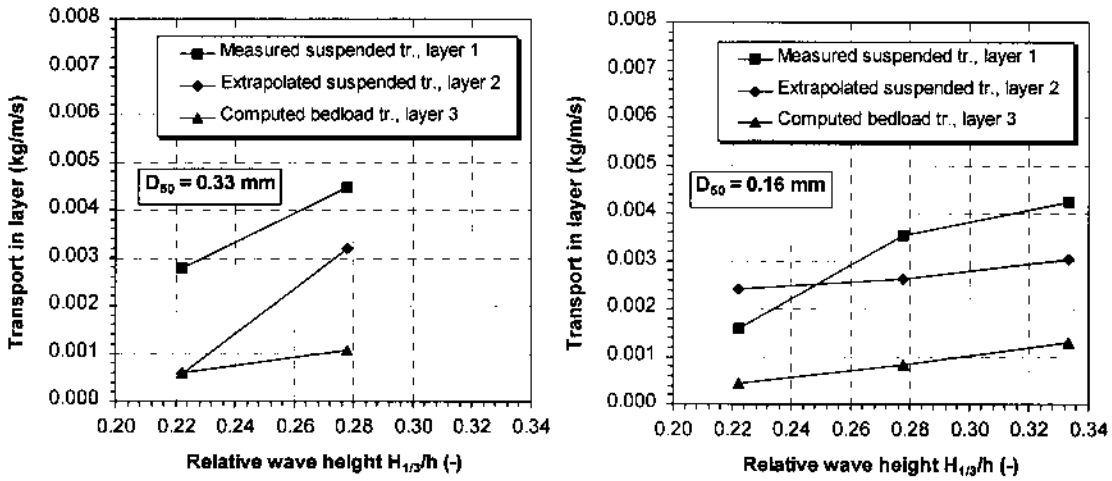

Fig. 6. High-frequency transport component in layer 1, 2 and 3 (left: D_{50}= 0.33 mm; right: D_{50}= 0.16 mm).

Modeling of high-frequency suspended sand transport

The high-frequency suspended load transport rates measured in the Delta flume were compared with a formulation proposed by Houwman and Ruessink (1996). The wave-related sand transport is defined as the transport of sand particles by the oscillating fluid components (cross-shore orbital motion). Houwman and Ruessink (1996) found that this high-frequency suspended load transport is an important component in the total net transport rate. In their approach the mean sediment concentration at a certain height above the bed is thought to be the time-averaged value of two sediment concentration peaks per wave cycle, one during the onshore directed wave motion and the other during the offshore directed wave motion. According to the velocity moments approach the shape of the sediment concentration peaks can be assumed to be equal to the shape of $|u(t)|^3$.

If it is also assumed that each half-wave cycle can be described with linear wave theory with different amplitudes but with equal duration, equation (4) is derived.

$$\bar{c}(z) = k\left[\left|\frac{2}{T}\int_0^{T/2} U_{on}^3 \sin^3 \omega t\, dt\right| + \left|\frac{2}{T}\int_{T/2}^{T} U_{off}^3 \sin^3 \omega t\, dt\right|\right]$$
$$= k\left[U_{on}^3 + U_{off}^3\right]\left|\frac{2}{T}\int_0^{T/2} \sin^3 \omega t\, dt\right| \qquad (4)$$

In equation (4), the left term is the time-averaged sediment concentration at height z above the bed, U_{on} and U_{off} refer to the onshore and offshore peak orbital velocity, T and ω are the wave period and angular frequency respectively and k is a constant.

The oscillatory suspended sediment transport at a certain height z above the bed can be related to the fourth order moment $u^*|u^3|$. The wave-averaged oscillatory sediment transport rate S(z) through a layer dz is then described by:

$$S(z) = \frac{1}{T}\int_0^T k\, u(t)|u(t)^3|dt$$
$$= k\left[U_{on}^4 - U_{off}^4\right]dz * \frac{1}{T}\int_0^{T/2} \sin^4 \omega t\, dt = k'\,\bar{c}(z) * \frac{U_{on}^4 - U_{off}^4}{U_{on}^3 + U_{off}^3} \qquad (5)$$

with:

$$k' = \frac{1}{2}\int_0^{T/2} \sin^4 \omega t dt \left(\int_0^{T/2} \sin^3 \omega t dt\right)^{-1} = \frac{9\pi}{64} \approx 0.44 \qquad (6)$$

After integration over the vertical the oscillatory suspended sediment transport is obtained. This approach gives an upper limit for the suspended oscillatory sediment transport, assuming that there are no phase lags between u(t) and c(t) and that the sediment always responds instantaneously to the third power of the orbital velocity, which always results in an onshore directed oscillatory suspended sediment transport rate. However, both field (Houwman and Ruessink, 1996; Vincent and Green, 1990) and laboratory measurements (Grasmeijer and Van Rijn, 1999) have shown that phase lags are present, sometimes even resulting in an offshore directed oscillatory suspended transport rate. For the efficiency coefficient k' this may result in smaller or even negative values.

Houwman and Ruessink (1996) determined the k' coefficient based on mean concentrations computed using the VanRijn/Ribberink model, and measured significant onshore and offshore orbital velocities. Comparison with the theoretical coefficient k' showed that the observed efficiency coefficient was significantly smaller than the theoretical value. The observed efficiency coefficient ranged from 0 to 0.2 instead of having a fixed value of 0.44.

In contrast with Houwman and Ruessink (1996), in the present study the k' value was determined from measured concentrations. Time-averaged concentrations measured with the ASTM were integrated between the lowest and the highest

measurement point (between 0.075 and 1.075 m above the bed). Measured significant onshore and offshore peak orbital velocities ($U_{1/3,on}$, $U_{1/3,off}$) were used in Equation (4), in correspondence with Houwman and Ruessink. The k' value might depend on wave height, bed material and bedforms. These effects are not taken into account here. Therefore, tests with the same wave conditions, bed material and bedforms were averaged to prevent biasing. Using a least square method an optimum value of k' = 0.3 was found.

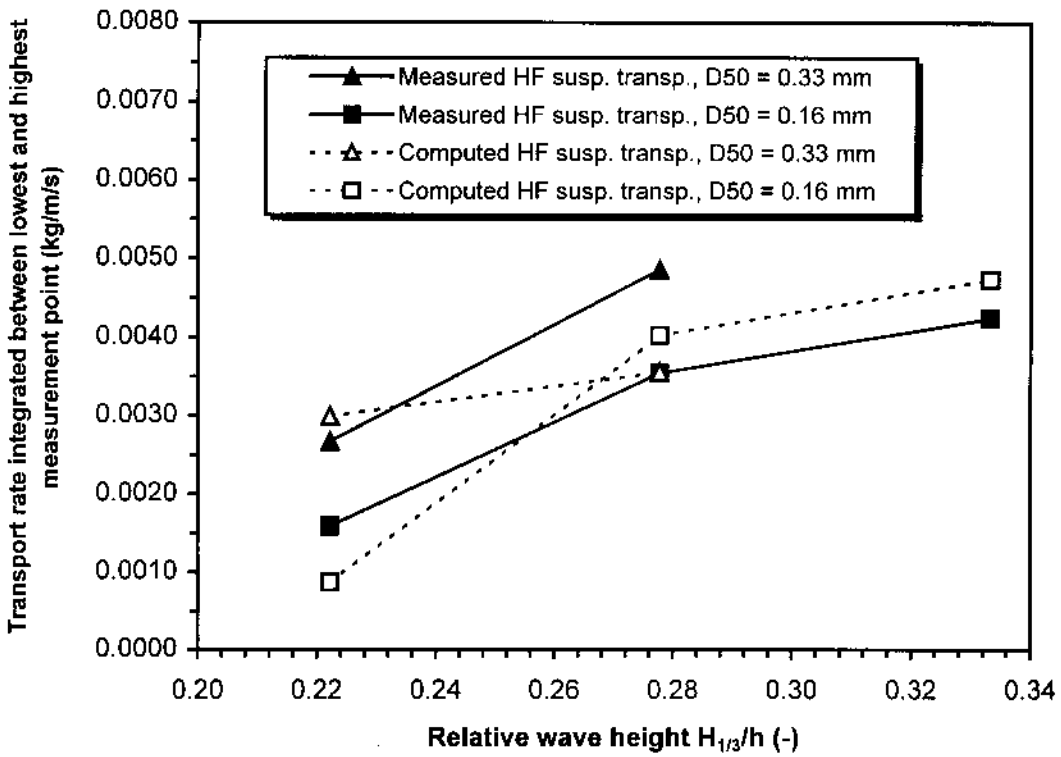

Fig. 7. Measured and computed high-frequency suspended transport rate as a function of relative wave height.

Figure 7 shows the measured and computed high-frequency suspended transport rates (using k' = 0.3) as a function of significant wave height. The data shown in Figure 7 are averaged values in layer 1 using tests with corresponding wave conditions and bed material. On an average the standard error between the tests was found to be about 30%. It is interesting to see that the high-frequency suspended transport rates for coarse sand are larger (factor 1.5 to 2) than for fine sand. This may be related to the presence of relatively large and steep ripples in case of coarse sand (mean ripple height: ± 0.05 m, mean ripple length: ± 0.23 m). For fine sand the mean ripple height and length were found to be approximately 0.005 m respectively 0.70 m.

It can be observed from Figure 7 that the increase of transport rate with wave height is overestimated by the Houwman method in case of fine sand and underestimated in case of coarse sand. This might be caused by dependence of the efficiency coefficient k' on wave conditions, bedforms or bed material. The efficiency coefficient might also change with height above the bed.

Using a different type of analysis Ruessink et al (1998) show the efficiency coefficient to be dependent both on the relative wave height and on the height z above the bed. The efficiency coefficient k' can be seen as a measure for the coherence between the velocity and the concentration signal, based on cross-spectral analysis. Ruessink et al (1998) found the coherence between the oscillatory components of measured velocity and concentration to be insignificant at all frequencies for $H_{1/3}/h < 0.29$ and $H_{1/3}/h < 0.35$ at elevations $z = 0.15$ m and $z = 0.25$ m above the bed, respectively. Measurements under more energetic conditions showed significant coherences between velocity and concentration around the wave spectrum peak period. The coherence decreased with height above the bed.

To evaluate the k'-coefficient over a wider range of conditions additional measurements for $H_{1/3}/h$ in the range of 0.3 to 0.6 are required.

TOTAL LOAD TRANSPORT RATE

Field experiments Egmond aan Zee

Field measurements near the coast of Egmond aan Zee, the Netherlands, were conducted in order to study the depth-integrated sand transport rates at different locations across the inner nearshore bar.

The study area is part of the Holland coast, which was described extensively by Wijnberg (1995). The Holland coast is an inlet free, wave dominated, coast, which mainly consists of sandy beaches and multiple barred nearshore zone. The length of this coastline is about 120 km and the orientation of the slightly curved coastline is essentially NNE-SSW.

The study area is located near Egmond aan Zee, the Netherlands. The tidal range near Egmond aan Zee varies between 1.2 m (neap tide) and 2.1 m (spring tide). During the experiments the nearshore zone of this area was characterized by two subtidal nearshore bars. The outer nearshore bar, a longshore uniform, straight bar, oriented parallel to the shoreline, was located at 550m offshore. The inner nearshore bar, a non-straight longshore bar, was located at 200 m offshore. The sediments in the study area are well sorted and composed of fine to medium sand with a median grain size between 250 and 350 μm.

Measurements of wave height, velocity, and sediment concentration at four or five locations in a cross-shore array over the inner nearshore bar were performed using the Coastal Research Instrumented Sledge (CRIS), which was pulled by the WESP. The WESP is a large multi-purpose vehicle. The design was derived from the Coastal Research Amphibious Buggy (CRAB) constructed by the US Army Corps of Engineers. The CRIS is a 3.5 m square and 2.5 m high carriage. Instruments mounted on the CRIS included a pressure sensor, three electromagnetic velocity meters, the ASTM, three OBS's and a ripple profiler. Sand transport measurement were performed at eight elevations above the bed from 0.02 to 1.0 m. The instruments were mounted on an outrigger extending 3 m seawards from the backwheels of the CRIS. The instruments could be adjusted at a given elevation above the bed with an accuracy of ± 0.01 m using a vertically movable arm. Dependent on the conditions, 8.5 or 17.1 minute long records were obtained. In order to minimize the influence of settling of

the CRIS into the bed, measurements were started 25 minutes after the CRIS was placed in position. Consequently, each measurement position took about 1 hour of time. Additional measurements were performed using four instrumented tripods positioned in a cross-shore array over the inner nearshore bar.

The depth-integrated suspended transport rate ($q_{suspension}$) was determined using the measured time series of velocity and concentration. The near-bed transport rate (q_{bed}) was determined using Equation (3).

In this paper, CRIS measurements performed on 2 May 1998 will be discussed. On 2 May, measurements were done at five locations across the inner nearshore bar (Figure 8): two at the seaward slope of the inner nearshore bar, one at the crest of the inner nearshore bar, and the last measurement position was located at the landward slope of the inner nearshore bar.

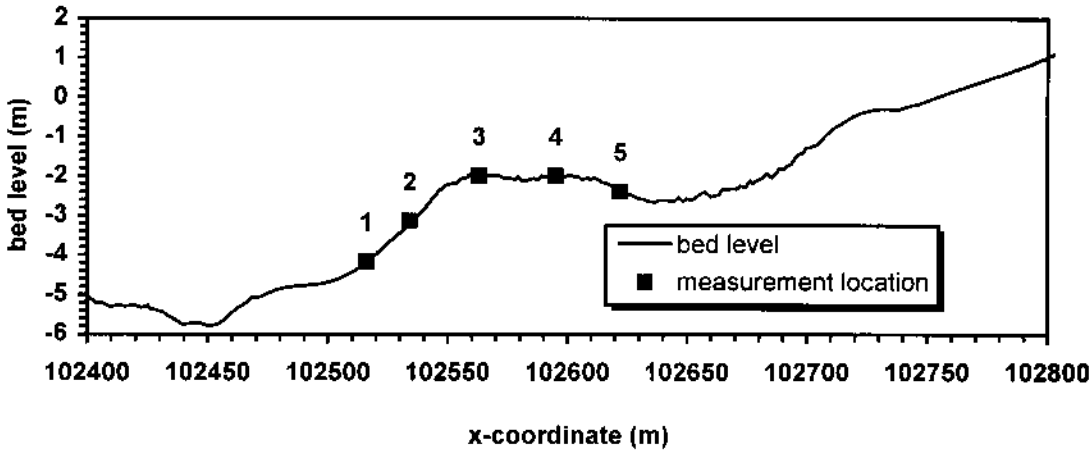

Fig. 8. Measurement locations on 2 May 1998.

Measurements with an instrumented tripod positioned at the seaward flank of the inner nearshore bar showed that the significant wave height during the period between the first and the last CRIS measurement was approximately constant at 1.25 m, while the tide level decreased from 1.21 m to 0.27 m NAP (Dutch ordnance level). Consequently, the CRIS measurements can only be compared based on local and temporal conditions. At the measurement locations the mean water depth ranged from 5.3 m to 2.5 m. Significant wave heights ranged from 1.0 to 1.2 m. Relative wave heights ($H_{1/3}/h$) are shown in Figure 9. Waves were non-breaking at locations 1 and 2. Waves were breaking at locations 3, 4 and 5, with fractions of breaking waves of respectively 15, 45 and 11 %. The waves started breaking at the landward side of the bar crest but continued breaking over several wave lengths while propagating further landwards. Thus, waves initially breaking at the seaward side of the bar crest were also included in the fraction of waves breaking at locations further landwards. The peak period was 7.0 s (± 0.3 s). Analysis of nearshore profiles measured on 2 May and on 3 May 1998 with the WESP hardly showed any morphological changes of the inner nearshore bar.

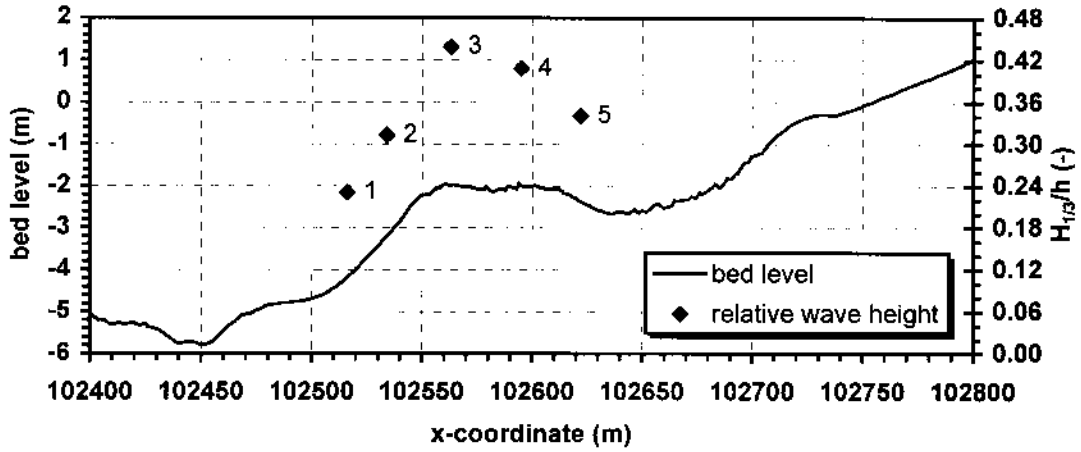

Fig. 9. Relative wave height ($H_{1/3}$/h) at different measurement locations

The depth-integrated suspended transport rates (between the lowest and the highest measurement point) and the computed transport rate in the unmeasured zone near the bed at different locations across the inner nearshore bar are presented in Figure 10. It can be observed that the time-averaged suspended transport rate (Qxa) is offshore directed at all measurement locations. The high-frequency oscillatory suspended transport rate (Qxss) is onshore directed at measurement locations 1 to 4 and of the same order of magnitude as the time-averaged component. At location 5 the high-frequency suspended transport component is negligibly small. The low-frequency suspended transport component (Qxll) is negligible at all measurement locations.

It can also be observed from Figure 10 that the transport rate in the unmeasured zone near the bed (Qb) is of the same order of magnitude as the net suspended transport rate and sometimes even larger.

This finding stresses once more the fact that the sand transport in the unmeasured zone can not be neglected. As this latter transport component can not be measured directly, it should be estimated from measured instantaneous velocities near the bed using an appropriate bedload transport formula.

CONCLUSIONS AND RECOMMENDATIONS

The main conclusions of this study are summarized as follows:

- The bedload transport rate in the wave tunnel could be predicted with reasonable accuracy using a relatively simple bedload transport formulation.
- The high-frequency suspended transport rate could reasonably be predicted using the modified Houwman method
- The most important components in determining the direction and the magnitude of the net suspended transport rate (Qx) are the time-averaged suspended transport component (Qxa) and the high-frequency suspended transport component (Qxss).
- In field conditions the transport rate in the unmeasured zone near the bed (Qb) was found to be of the same order of magnitude as the net suspended transport rate, sometimes even larger.

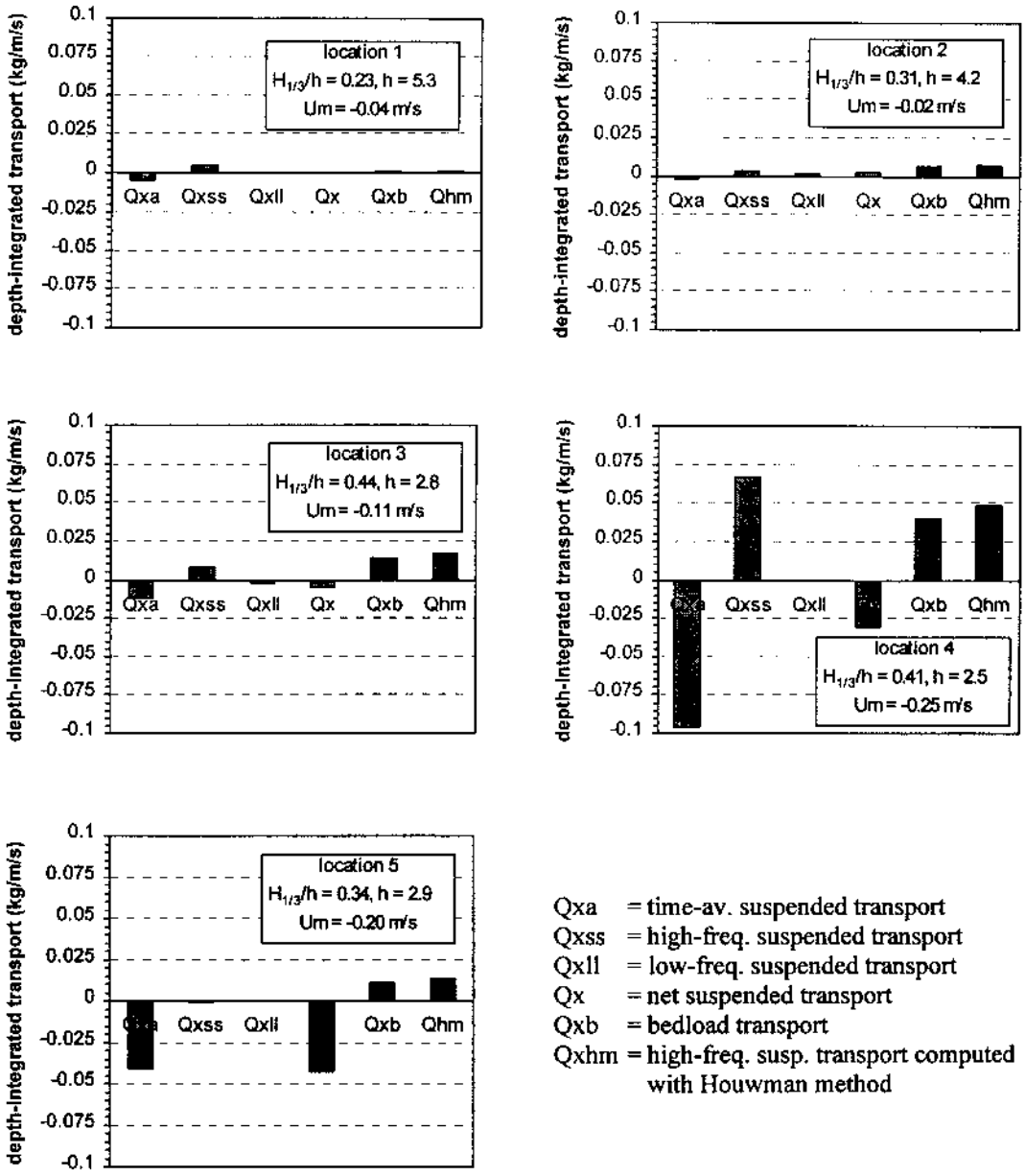

Fig. 10. Depth-integrated suspended load transport rates and bedload transport rates.

ACKNOWLEDGEMENTS

The authors are grateful for having had the opportunity to participate in the LIP-tests 1998 in the Delta flume of Delft Hydraulics; especially the scientists of the Proudman Oceanographic Laboratory in Bidston (England) are gratefully acknowledged for the pleasant cooperation. Jan Mulder of RIKZ is acknowledged for sponsoring of the experiments in the wave tunnel and the Delta flume. This work was undertaken as part of the Coast3D project funded by the European Commission's research program MAST under Contract Number MAS3-CT97-0086.

REFERENCES

Dang Huu, Ch., B.T. Grasmeijer and L.C. van Rijn, 1999. Analysis of sand transport under regular and irregular waves in a large scale wave flume. Univ. of Utrecht, the Netherlands.

Houwman, K.T. and G. Ruessink, 1996. Cross-shore sediment transport mechanisms in the surfzone on a timescale of months to years, Proc. Coastal Engineering 1996, pp.4793-4806, ASCE, New York.

Huntley, D.A. and D.M. Hanes, 1987. Direct measurement of suspended sediment transport, Proc. Coastal Dynamics 1987, pp. 723-737, ASCE, New York.

Janssen, C.M., W.N. Hassan, R.J. van der Wal and J.S. Ribberink, 1996. Net sand transport rates and transport mechanisms of fine sand in combined wave-current sheet flow conditions, *Report H2462*, part IV, Delft Hydraulics, Delft, The Netherlands.

Osborne, P.D. and B.G. Greenwood, 1992. Frequency-dependent cross-shore suspended sediment transport. 2; a barred shoreface. Marine Geology 106, pp. 25-51

Osborne, P.D. and C.E. Vincent, 1996. Vertical and horizontal structure in suspended sand concentrations and wave-induced fluxes over bedforms. Marine Geology, Vol. 131, pp. 195-208

Ribberink, J.S., 1998. Bedload transport for steady flows and unsteady oscillatory flows. Journal of Coastal Research, Vol 34, pp. 59-82

Ribberink, J.S. and A. Al-Salem, 1991, 1992. Sediment transport, concentrations and bed forms in simulated asymmetric wave conditions, *Report H840*, parts IV, V and VI, Delft Hydraulics, Delft, the Netherlands.

Ruessink, B.G., K.T. Houwman, P. Hoekstra, 1998. The systematic contribution of transporting mechanisms to the cross-shore sediment transport in water depths of 3 to 9m. Marine Geology 152, pp. 295-324

Vincent, C.E. and M.O. Green, 1990. Field measurements of the suspended sand concentration profiles and fluxes and of the resuspension coefficient over a rippled bed" Journal of Geophysical Research Vol. 95 (C7). pp. 11591-11601.

Wijnberg, K.M. 1995. Morphologic behaviour of a barred coast over a period of decades. *Ph.D. thesis*, Univ. of Utrecht, the Netherlands, 245 pp.